Supporting Information

Prasad *et al.* 10.1073/pnas.0805981105

SI Text

I. Basic Signaling Model

I.1 Description of Signaling Model 1. The signal strength is represented by the number of activated Zap70 molecules at the start of the simulation (1, 2).

2. ZAP70 phosphorylates LAT (3). LAT has three phosphorylation sites. These will be referred to as Y132, Y191, and Y226. The phosphorylation rules are as follows.

3. Y132 requires either Y191 or Y226 to be phosphorylated before it can be. Both Y191 and Y226 are phosphorylated independently (4, 5). Such a cooperative phosphorylation can arise owing to a conformational change in LAT due to phosphorylation at Y191 or Y226 that facilitates phosphorylation at Y132. In accordance with this, we also assume that if the species with only a phosphorylated Y132 site forms owing to dephosphorylation reactions, it is unstable and decays with a fast rate.

4. Upon being phosphorylated, Y132 binds PLCγ1 exclusively. Y191 and Y226 bind both Gads and Grb2, although with different binding affinities. We have used the measured *in vitro* affinities reported in Houtman *et al.* (6).

5. If PLCγ1 is bound to Y132, then Gads binds stronger to Y191 and stabilizes PLCγ1 (4, 6, 7). This is implemented by having a lower off-rate for the unbinding of both Gads and PLCγ1 in this situation than for either of them singly.

6. If Gads is bound to Y191, then Grb2 binds stronger to Y226 (and *vice versa*) and stabilizes Grb2 on Y226 (4, 6, 7). This is implemented by the same method as above.

7. If PLCγ1 is bound to Y132, Gads to Y191, and Grb2 to Y226, then cooperative interactions stabilize the entire complex (6, 7). This complex dissociates into its parts by a uniform off-rate that is lower than any of the single off rates. We refer to this complex as the *complete complex*.

8. Gads (Itk) on Y191 is required for the activation of PLCγ1 on Y132. Active PLCγ1 can deactivate via the generic phosphatase or by unbinding. This follows from the reports that Gads is constitutively associated with SLP76-Vav-Itk (8), and Itk activates PLCγ1 (9).

9. We assume high concentrations of a phosphatase that dephosphorylates all species except ZAP70. We assume that ZAP70 decays by a slow first-order process.

10. We assume that SOS is constitutively bound with Grb2 (10) and that Grb2-SOS can activate RasGDP only when bound to LAT, because that is the step required to bring SOS to the plasma membrane (10).

11. We assume that if the allosteric site is empty, the catalytic site of Grb2-SOS neither binds to nor catalyzes RasGDP. We similarly ignore the spontaneous conversion of RasGDP to RasGTP. Both of these have been measured to be approximately the same level (11). Because in our simulations the concentration of RasGDP is much higher than that of Grb2-SOS, almost all Grb2-SOS on LAT will be bound to RasGDP or RasGTP. Therefore at any level of signal, the contribution of the basal rate of Grb2-SOS in generating RasGTP will be negligible. Thus this simplifying assumption is not likely to have any qualitative effect on the model.

12. When RasGDP or RasGTP is bound to Grb2-SOS on the allosteric site, it is catalytically active. We use parameters reported by Kuriyan *et al.* (11–13) for the cases when RasGDP or RasGTP are bound to the allosteric site of SOS. We assume (to keep the system size small) that when RasGDP is bound to the catalytic site, RasGDP or RasGTP that is present at the allosteric site does not unbind. Because bare SOS has by assumption no catalytic activity, this simplification has no qualitative effect on the model results.

13. Phosphorylated PLCγ1 bound to LAT can cleave PIP2 into DAG and IP3 (14). DAG binds with Rasgrp1 to activate it. Rasgrp1 catalytically transforms RasGDP into RasGTP (15). Along with RasGTP, this reaction produces a marker molecule that allows us to keep track of the production of activated Ras by this pathway.

14. The membrane contains a constitutive concentration of RasGAP's that catalytically transform RasGTP back to RasGDP.

Description of the Biochemical Network

In accordance with the above rules, the following steps can happen in the reaction network.

1. Zap70 binding, unbinding, and phosphorylation of LAT.
2. Phosphotase binding, unbinding, and dephosphorylation of LAT.
3. Grb2/SOS binding and unbinding with LAT.
4. PLCγ1 binding and unbinding with LAT.
5. Gads binding and unbinding with LAT.
6. Gads activates PLCγ1 on LAT.
7. Activated PLCγ1 can unbind from LAT, or bind to, unbind from, or hydrolyze PIP2, producing DAG and IP3.
8. RasGRP binds with DAG.
9. RasGRP bound to DAG on the plasma membrane (PM) catalyzes nucleotide exchange of RasGDP, creating RasGTP and a marker molecule.
10. Grb2/SOS binds RasGDP or RasGTP on the allosteric site.
11. Grb2/SOS complexed with RasGDP or RasGTP on the allosteric site binds to or unbinds from RasGDP on the catalytic site.
12. Gbr2/SOS bound to RasGDP on the catalytic site catalyzes nucleotide exchange producing RasGTP.
13. RasGAPs bind to, unbind from, and deactivate RasGTP and the marker molecule.
14. Species containing complexes only on Y132 that cannot form directly, decay if formed by any sequence of reactions in the network.

The system consists of 3364 chemical reactions and 549 species. The parameter values used for the reaction types described above are reported in Table S1 and the concentrations in Table S2.

To check whether the simplifying assumptions in I.1.3 and I.1.12 have any qualitative effect on our model, we constructed a larger model with these assumptions relaxed. Simulations of the Ras signal in the larger model showed no qualitative difference with the results obtained by our base model (data not shown).

I.2 Stochastic Simulations of the Chemical Master Equations The model consists of a network of chemical reactions defined by the above description of the model rules. To solve these systems of chemical reactions we use the Gillespie algorithm to carry out stochastic simulations of these reactions (16). The fundamental advantage of performing stochastic simulations of the chemical reaction master equations over the more traditional method of using systems of ordinary differential equations is because chemical reactions in reality are neither continuous nor deterministic, as assumed by the latter method. Use of exact stochastic

simulations therefore allows us to examine the possible effects of noise and fluctuations in the system.

The stochastic simulations are performed in the following way. We assume a certain number of reactant molecules, in a reaction volume pictured in Fig. S1. It can be shown that the waiting time distribution of reactions in this volume is exponential, whereas the probability of the occurrence of each reaction is given by its relative propensity (i.e., reaction rate multiplied by the concentration expressed as the ratio of the sum of such propensities for all reactions). The first provides the time step of the simulation, whereas the second provides the method of choosing the reaction that occurs at the time step (16). This process is repeated for a specified time. The concentrations after a fixed number of time steps are recorded to produce the time traces shown later. Alternatively, the concentrations in a time window are averaged to produce the average output for that time.

The molecules LAT, PIP2, DAG and Ras are all membrane bound. ZAP70 is also considered membrane bound because it is usually associated with the TCR and CD3 ζ chains while activated. The other molecules (i.e., RasGAP, Rasgrp1, PLCγ1, Gads, and Grb2) are cytosolic. We assume that when a cytosolic molecule comes within a distance d of the membrane, it can react with membrane-bound molecules. In these simulations we have taken d = 1.7 nm, which is the radius of gyration of a Ras molecule (17). The area of the PM in the box has been taken to be 4 μm^2 and the total depth 20 nm, yielding a volume of V_{3d} = 0.08 μm^3. The volume inhabited by the membrane-bound molecules is thus V_{2d} = 0.0068 μm^3.

The Gillespie simulation method assumes that the simulation volume is well mixed. This is a reasonable assumption provided association on-rates for a bimolecular reactions are smaller than the diffusional on-rate. The diffusion constant of activated ZAP70 at the membrane (18) is approximately 0.2 $\mu m^2 s^{-1}$. Diffusion constants of Ras molecules or cytosolic species are larger by an order of magnitude or more. Using these numbers, we can make an estimate of the diffusional rate of encounter between two protein molecules, using the well-known formula for diffusion limited reaction rates,

$$k_{diff} = \frac{4\pi N_0}{1000}(D_A + D_B)(r_A + r_B), \qquad [1]$$

where N_0 is Avogadro's constant, D_A and D_B are the diffusion rates of the two molecules, r_A and r_B are their radii in cgs units, and k_{diff} is in $M^{-1}s^{-1}$. The slowest association reaction in our system is most probably that between ZAP70 and LAT. Using 10 nm as the sum of the radius of the proteins and 0.2 $\mu m^2 s^{-1}$ as the sum of their diffusion constants, we get k_{diff} is = 15 $\mu M^{-1}s^{-1}$. An encounter between LAT and a cytosolic molecule like PLCγ1 is likely to have a much larger collisional on-rate (owing to the higher cytosolic diffusion constant of approximately 1–10 $\mu m^2 s^{-1}$ (19), and the on-rate between a lipid and a membrane-bound protein can be expected to be of a similar order of magnitude owing to the smaller lipid size and diffusion coefficient of approximately 1 $\mu m^2 s^{-1}$ (20). These rough estimates lead to the expectation that spatial effects are unlikely to be significant, provided we use the appropriate diffusion-limited on-rate as an upper bound for the association rate in the simulation. It can be seen from Table S1 that all on-rates in the simulation are in fact lower than the slowest on-rate calculated above.

Note also that decreasing on-rates by a factor of 5 has no qualitative effect on the results (see sensitivity analysis below). Hence we do not expect any contribution from spatial effects to qualitatively alter our conclusions.

For binding reactions the Gillespie rate is obtained from the on-rate by dividing by the simulation volume. However, there are three types of possible binding reactions in the simulation box, between two species anywhere on the box (3d−3d), between two species on the plasma membrane (2d−2d), or between a membrane-bound species and a cytosolic species (2d−3d). In a homogeneous Gillespie simulation, the appropriate way to take these differences into account is by transforming the reaction rate differently.

For the reaction $A + B \rightarrow C$, for example, the law of mass action leads to the mean-field equation,

$$\frac{d[C]}{dt} = -k[A][B], \qquad [2]$$

where $[A]$ *etcetera* implies the concentration of the species A, and k is the reaction rate. If both the species are cytosolic, the concentrations can be written $[A] = N_A/V$ *etcetera*, where N_A is the number of molecules of type A. In terms of numbers of molecules, therefore, the mean field equations become,

$$\frac{dN_C}{dt} = \frac{k}{V}N_A N_B. \qquad [3]$$

Thus the appropriate Gillespie rate for the simulation is k/V.

If all three species are membrane bound, we assume that they live in a rectangular slab of thickness d (see Fig. 1) and volume V_{2d}. For the Gillespie simulation, this implies that the probability of encounter of A with B must be rescaled appropriately to take into account this smaller volume. Carrying out the procedure above yields the equation,

$$\frac{dN_C}{dt} = \frac{k}{V_{2d}}N_A N_B, \qquad [4]$$

indicating that the enhanced probability of encounter can be taken into account by choosing the Gillespie on-rate as k/V_{2d}. Note that here we assume that 2d reactions can be thought of as 3d reactions in a thin slab and are ignoring the issues connected with defining a reaction rate in two dimensions. For 2d−3d reactions we take the lack of symmetry of the species into account by writing the concentrations of the 2d species, say A, as

$$[A] = \frac{N_A}{V_{2d}}\theta(z + d), \qquad [5]$$

where $\theta(x) = 0$ if $x < 0$ and $\theta(x) = 1$ if $x \geq 0$, and the origin of the axes is assumed to be at the top left-hand corner of the simulation box. Writing down the mean-field equations in this terminology, elementary algebra shows that the Gillespie rate is again k/V as in the 3d−3d case.

I.3 Changes in the Simulation Volume It is of interest to ask whether any of the qualitative characteristics of our model is affected by the choice of the simulation box volume. To test whether this has any effect, we ran the simulation again after changing the volume by a factor of 0.5, 1.5, and 2 and compared it with the base case. The concentrations were kept the same, hence the number of molecules in the simulation box and the forward rates of the reactions were changed by the appropriate factors. We found that whereas changing the volume keeping concentrations fixed changes the threshold number of molecules of ZAP70 required to initiate the positive feedback loop in Ras activation (Fig. S1*A*), plotting the results in terms of concentrations makes all of the curves fall on the same line (Fig. S1*B*), showing that there is no difference on changing the simulation volumes.

I.4 Parameter Sensitivity Analysis 1. Differential sensitivity analysis was carried out for each kinetic parameter with respect to the output of RasGTP at the base vector of parameter values. The

fully normalized sensitivities are defined as follows. The sensitivity coefficient S_{ij} of species y_i with respect to parameter k_j is:

$$S_{ij}(t) = \frac{\partial \ln y_i}{\partial \ln k_j} \approx \frac{\Delta y_i / y_i}{\Delta k_j / k_j} \quad [6]$$

The sensitivity coefficient we calculated measures the percentage change in output of RasGTP with respect to a percentage change in a parameter value and is a function of time. Most parameters showed sensitivity coefficients of less than 1 for all times; the few that exceeded this number showed higher sensitivity at very early times (when concentration of RasGTP would be very low). Because these sensitivities display no unusual instability of the model with respect to any parameter, they are not being reported here.

2. We then varied each reaction rate parameter by a large discrete change, first decreasing it by a factor of 5 and then increasing it by a factor of 5, and ran the simulation again to assess the effect of the change on the RasGTP signal. If a measurement of a dissociation constant was available, then we varied both the on-rate and the off-rate while keeping the measured dissociation constant unchanged. All other reaction rates, including those for which measurements exist, were varied independently by the same factors (Table S3).

The figures that follow contain the results summarized in Tables S3 and for selected cases provide more insight into the kinetics of Ras activation at these parameter values.

We also carried out parameter sensitivity analysis by varying all parameters randomly by 20%. This checks to determine whether nonlinear effects can affect the qualitative results that we present. Details of the results of this analysis are presented in Section I.3.2.

For both of the above methods of sensitivity analysis we obtained the set of conditions on our model that yield the desirable qualitative results. These conditions can be stated as follows:

1. We require a positive feedback loop in Ras activation by SOS as described. However, the highest catalytic rate of SOS should be sufficiently greater than the catalytic rate of Ras activation by RasGRP.

If the catalytic rate due to RasGRP is larger than that due to SOS, RasGRP activates all of the RasGDP present in the simulation volume before SOS has had a chance to be recruited on the membrane and its positive feedback loop activated.

2. The GTPase activity of RasGAPs must not suppress weaker Ras activation through RasGRP. However, the GTPase activity of RasGAPs must not be so low that RasGRP activates most Ras molecules in the simulation volume.

If RasGAPs suppress weak Ras activation via RasGRP and the smaller SOS rate, the positive feedback loop in SOS cannot ignite. However, if RasGAP activity is very weak, it can allow RasGRP to activate all Ras molecules in the simulation before the SOS positive feedback loop has been activated. Note that in reality RasGAPs are dynamically modulated, so this condition is expected to be less stringent in the biological system than in our model.

3. Cooperative complex formation at the LAT signalosome must be required and stable enough for efficient Ras activation by SOS.

Impairing the stability of the Ras signalosome does not allow SOS enough time to activate the positive feedback loop. However, if cooperative complex formation is not required for stable recruitment of Grb2/SOS, weak signals will also activate the positive feedback loop.

As shown in the main article, all of these conditions are supported by experimental observations.

Note on Figures for Parameter Sensitivity Analysis The plots of total RasGTP from the simulations carried out for the parameter sensitivity analysis are presented in Figs. S1*C*−S4*C*. The symbols b and u in the legends imply binding−unbinding reactions of the species mentioned; cat implies catalytic reactions. Thus "b/u" is the binding−unbinding pair when parameters have been changed in tandem.

Variation of Concentrations

Basis for Concentration Estimates Presented in Table S2. None of the concentrations of the molecules in our model have been measured in lymphocytes, let alone in thymocytes. Prior computational studies of different cells have used guesses for most of these concentrations, whereas only some have been measured. Measured values of some important molecules like Ras vary widely for different cell types. We have therefore used plausible estimates of concentrations for our simulations and subjected them to sensitivity analysis by varying each concentration by a factor of 4, discussed below. Our estimates for different species are arrived at in the following manner. No measurements of LAT concentration exist in the literature. Given the role of LAT in early signaling events, we thought it plausible to assume that LAT is present in approximately the same quantities, or maybe a little less, than the TCR. Because the concentration of the TCR has been measured at approximately 300 molecules/μm^2 (21), we chose an estimate of 250 molecules/μm^2 for LAT. Some measurements do exist for RasGDP, and a recent measurement found that RasGDP in HeLa cells was approximately 0.4 μM (and 0.5 μM in COS cells) (22). Using the former number and the reported dimensions of the HeLa cell, we obtain a RasGDP concentration of approximately 450 molecules/μm^2. However other estimates report much smaller concentrations (22). We therefore used a value within the range of measured concentrations for RasGDP. An estimate for the concentration of Grb2 in another mammalian cell is 1 μM (23). (Note that this is an estimate and, as far as we could ascertain, not a measurement.) In order for signaling clusters to form efficiently on LAT, we chose concentration values for all of the three species—Grb2/SOS, Gads, and PLCγ1—to be approximately 2 μM, which is within a factor of 2 of the earlier estimate. Concentrations of PIP2 were based on estimates that it constitutes approximately 5% of membrane lipids (3). Concentrations of RasGRP were chosen on the basis of the requirement that RasGRP does not activate all of the RasGDP before the ignition of the SOS feedback loop, and concentrations of the RasGAPs were chosen that yielded an activation threshold of approximately 100 Zap70 molecules. Because it is widely believed that there is a large concentration of phosphatases in the cell (21), we chose a concentration that is five times that of Grb2/SOS. However, we also varied all concentrations by a factor of 4, and our model is robust to these changes (results below).

To check the sensitivity of our model to the concentrations chosen for the different signaling molecules, we varied all concentrations (except for ZAP70, which represents signal strength) by a factor of 2, greater and less than the base case. The effects of this variation are listed below.

1. LAT: There is no qualitative effect due to concentration change in either direction (Fig. S3*D*).

2. PIP2: There is no qualitative effect due to concentration change in either direction (Fig. S3*D*).

3. PLCγ1: There is no qualitative effect due to concentration change in either direction (Fig. S3*D*).

4. Grb2/SOS: Halving the concentration decreases the number of stably bound Grb2/SOS molecules at any signal strength. This implies that threshold of activation becomes larger and takes longer (Fig. S3 *D*−*F*). Increasing concentration decreases threshold for positive feedback initiation and makes it faster.

5. Gads: There is no qualitative effect due to concentration change in either direction (Fig. S3*G*).

6. RasGDP: There is no qualitative change when RasGDP concentration is halved (Fig. S3*G*). However when RasGDP concentration is doubled, it increases the propensity of SOS and RasGDP binding, thereby slowing the initiation of the positive feedback loop (Fig. S3 *G* and *H*).

7. RasGAPs: Halving the concentration causes the threshold of activation to fall (Fig. S3*G*). Doubling the concentration, on the other hand, suppresses the RasGTP signal. At this concentration, appreciable RasGTP production would require a larger concentration of RasGEFs. Increasing Grb2/SOS concentration restores activation (Figs. S3*G* and S4*A*).

8. Phosphotase: Halving the concentration decreases the threshold for the initiation of the positive feedback loop, whereas doubling it decreases the threshold for the same (Fig. S3*G*).

9. RasGRP1: Halving the concentration increases the threshold for initiation of the positive feedback loop, whereas doubling the concentration decreases the threshold for activation (Fig. S3*G*).

I.4.2 Changes in Multiple Parameter Values. We randomly changed all parameter values by 20% and ran several simulations. Although it is impossible to explore all of this parameter space (which consists of 2^{40} or 10^{12} possibilities), in the simulations we have performed we find that these small changes have a qualitative effect only when they strengthen the catalytic activity of RasGAPs while simultaneously reducing the strength of catalysis by either RasGRP or SOS (Fig. S4*B*). To check whether our explanation was correct, we reran all simulations that showed very low Ras activation with exactly the same parameter values except for the RasGAP rates. As expected, all cases show ignition of the positive feedback loop and maximal Ras activation under these conditions (Fig. S4*C*). One conclusion from this exercise is that the GTPase activity of the RasGAPs should not abrogate Ras signaling through RasGRP, otherwise the SOS feedback loop cannot be primed.

I.5 Phosphorylation of LAT In the model, the catalytic rate of LAT phosphorylation by ZAP70 and the rate of dephosphorylation by phosphatase together affect the kinetics of formation of fully phosphorylated LAT, and thereby the assembly of complete complexes. This is also accomplished by changes in concentration. We show below that increases in the rate of phosphorylation lead to a steeper increase in both total tyrosine on LAT as well as the number of fully phosphorylated LAT molecules.

I.6 Bimodality in RasGTP Signal In the base case considered in this paper, the RasGTP signal activates in approximately 20 min for a signal strength of approximately Zap70 = 250, above the activation threshold. The time window of 20 min for many of the observations in the article was chosen because of this behavior. However, although strong signals activate RasGDP in the simulation volume, the bimodal distribution of cells takes a longer time to be observed. At 20 min, for a typical signal strength in the bistable regime (Zap70 = 130), the distribution of RasGTP level has developed a long tail, which is a marker of the bistable positive feedback loop but is yet not bimodal (Fig. S5A, *Top*). At a time of 50 min, however, the distribution of RasGDP signal is bimodal. This time window is, however, much larger than the experimental observation time of the experiments reported in this article, which are less than 4 min.

The timing of the RasGTP signal is a complicated function of the parameters and concentrations, many of which are unknown. For example, other things remaining constant, reducing the concentration of RasGDP reduces the activation time significantly and leads to observation of bimodal behavior at 20 min (Fig. S5*B*, *Left*), which is more marked at 25 min (Fig. S5*B*, *Right*). The qualitative behavior of the signal is exactly the same as the base case we have considered (data not shown).

Furthermore, there are many uncertainties in the parameters, including those that have been measured *in vitro*, for which the *in vivo* rates may be somewhat different. We have shown below that our model is quite robust to significant changes in parameter values; however, what is affected by these changes are the kinetics and thereby the timing of activation. For example, if the rate of catalysis of SOS is higher by a factor of 5, the time taken for observing bimodality for signals a little above the threshold (Zap70 = 150) drops to approximately 8 min (500 s), shown in Fig. S5*C*. Finally, if the catalysis rate is increased by a factor of 5 and the concentration of RasGDP is decreased to 300 molecules, the activation time decreases even more. For a signal strength a little above the threshold in this case (Zap70 = 90 molecules), bimodality can be observed in 4 min (Fig. 5*A*). In all of these plots, apart from the changes mentioned, the only other change that needed to be done was small adjustments in the concentration of RasGAPs and the rate of DAG production. It is reasonable therefore to expect that suitable modification of additional parameters can yield activation in even faster times.

It should be noted, however, that there is one key difference between our simulations and reality in that there is no extrinsic noise in our system. Each simulation starts with an initial concentration that is the same for all runs. However, a glance at the distribution of active Erk at T = 0 in the experimental figure, Fig. 5*C* in the main text makes it evident that each cell is actually quite different from the others. Extrinsic noise can be expected in this case to add to intrinsic noise and amplify the bistability and increase the range of stimulatory strengths over which the bistability is observed.

Section II: Mutation Analysis

II.1 Description of Mutation Analysis The mutation analysis was performed in the following manner.

Gads-/-. Concentration of the species corresponding to Gads-SLP76-Itk was set to zero.

Y132F, Y191F, and Y226F. The forward rate for ZAP70 binding to these tyrosine sites was set to zero. This ensured that this tyrosine site was not phosphorylated and did not take part in any reactions in the model.

SOS-/-. To ensure that Grb2 was present but SOS was catalytically inactive, we set the forward rate of binding to the catalytic site of Grb2-SOS to be zero.

No Positive Feedback in SOS. We set the on-rate of RasGTP binding to the catalytic site of Grb2/SOS to be zero. Results of this simulation, not reported in the main text, are shown in Fig. S4 *F* and *G*.

II.2 Parameter Sensitivity of Mutations Parameter sensitivity analysis was conducted on all of the mutations. Parameters of binding−unbinding rates were changed in tandem; others were changed individually. Only those parameters were changed that were important in terms of the parameter sensitivity analysis of the main model, presented above. Results are tabulated in Table S4.

Note on Table S4. The threshold of Grb2/SOS at the membrane that is required for the initialization of the positive feedback and full activation of RasGTP is set by the interplay between the forward rates of the RasGEFs and the backward rate of the RasGAPs. Large decreases in the GTPase rate of the RasGAPs have the potential to lead to maximal activation of RasGTP even

at very low signal. Because of the significant effects of the RasGAP catalytic rate on the mutations, we also checked the effect of a more modest decrease in this rate. If the RasGAP catalytic rate is decreased by half, then the Gads-/-, Y132F, and Y191F mutations do not show significantly increased RasGTP activation over the level with the unaltered catalytic rate. However the SOS-/- mutation shows stronger activation of RasGTP via the RasGRP pathway. The NPF mutation shows an even stronger, although graded, activation of RasGTP (Fig. S4 *F* and *G*). As can be seen from Fig. S4*F*, the kinetics of Ras activation in this case are quite different from the base wild-type case because there is no sigmoidality or bistability in Ras activation. The Y226F mutation is the only one that shows full activation.

The above analysis suggests that depending upon the strength of the RasGAPs in the cell, the NPF mutation may not show full abrogation of negative selection but rather a graded response, in sharp contradistinction with the base case of digital negative selection. These predictions await experimental testing.

The Y226F mutation is physiologically complicated to interpret. In our model it represents Grb2 binding sites that are involved in cooperative interactions with Gads. However, Y191 is also a Grb2 binding site, so the Y226F mutation does not abolish Grb2/SOS recruitment on the membrane but abolishes stable binding, which in our model requires complex formation. Decreasing the rate at which Grb2/SOS unbinds from Y191 leads to stable binding even in the absence of complex formation. Because the Y226F mutation does not much affect the RasGRP pathway, increasing stable recruitment of Grb2/SOS on Y191 leads to ignition of the positive feedback loop and full activation. Full activation is also seen in this mutation on increasing the binding and unbinding rates of RasGTP on the allosteric site of SOS, as well as increasing the catalytic rates of both SOS with RasGDP and SOS with RasGTP on the allosteric site. The latter two changes have the effect of reducing the threshold of membrane-bound Grb2/SOS required for initiation of the positive feedback. The Y226F mutation is therefore qualitatively somewhat similar to the base model with reduced cooperativity, presented in Fig. S2*A-C*. These results indicate that elimination of one or two Grb2 binding sites on LAT would lead to a higher threshold for negative selection, but depending upon the physiological parameter values, this higher threshold may or may not be significantly different from the wild-type case.

Section III: Compartmentalization of Ras Signaling

III.1 Description of Signaling Model The compartment version of the model has the following features.

1. Rasgrp1 is activated by binding to IP3, which we treat as a surrogate for calcium. Activated Rasgrp1 binds to DAG on the membrane. It can also diffuse to the Golgi, where it binds to the DAG already present there. This is represented by a first-order reaction that transforms activated Rasgrp into an activated enzyme that acts on the RasGDP present on the Golgi. The rate of this first-order reaction is proportional to the time scale of diffusion to the Golgi and the concentration of DAG on the Golgi.

2. In the Golgi compartment, Ras is a separate species from that on the plasma membrane. The Golgi form of Rasgrp1 then catalytically transforms RasGDP into RasGTP with the same rates as on the membrane. In line with the suggestion by some experimental groups (2), the Golgi does not contain RasGAPs. This also, potentially, can lead to sustained Ras activation on the Golgi.

3. Along with a constitutive concentration of RasGAPs on the plasma membrane as before, there is a signal-activated pool of RasGAPs. This is implemented by using IP3 as the marker for the signal and introducing a new species that represents inactive RasGAPs. When this new species binds with IP3 produced by the signal, it becomes a catalytically active GTPase.

The additional parameters used for this simulation are presented below.

1. RasGRP binds to IP3 with a forward rate of 48.0 $\mu M^{-1}s^{-1}$ and an unbinding rate of 0.1 s^{-1}.

2. RasGRP free or complexed with IP3 binds with DAG with a forward rate of 4.08 $\mu M^{-1}s^{-1}$ and an unbinding rate of 0.08 s^{-1}.

3. RasGRP bound with IP3 translocates to the Golgi with a forward rate of 0.1 s^{-1}.

4. Golgi-limited RasGRP binds with Golgi-limited RasGDP with a forward rate of 0.32 $\mu M^{-1}s^{-1}$ and an unbinding rate of 1.0 s^{-1} (same as base case on PM).

5. RasGRP on the Golgi catalyzes RasGDP to RasGTP with a rate of 0.01 s^{-1} (same as on the PM).

6. Inactive RasGAP binds to IP3 and becomes active RasGAP with a forward rate of 0.48 $\mu M^{-1}s^{-1}$.

The compartment model shows the sharp response to ligand potency as shown by the main model but also naturally leads to Ras activation via RasGRP, being mostly at the Golgi and Ras activation by SOS confined to the plasma membrane (Figs. 5 *D*−*F*). This may potentially explain some of the compartmentalization results reported in the paper by Daniels *et al.* (2).

1. Houtman JC, Houghtling RA, Barda-Saad M, Toda Y, Samelson LE (2005) Early phosphorylation kinetics of proteins involved in proximal TCR-mediated signaling pathways. *J Immunol* 175:2449–2458.
2. Daniels MA, *et al.* (2006) Thymic selection threshold defined by compartmentalization of Ras/MAPK signalling. *Nature* 444:724–729.
3. Wange RL (2000) LAT, the linker for activation of T cells: A bridge between T cell-specific and general signaling pathways. *Sci STKE* 2000:RE1.
4. Zhu M, Janssen E, Zhang W (2003) Minimal requirement of tyrosine residues of linker for activation of T cells in TCR signaling and thymocyte development. *J Immunol* 170:325–333.
5. Lin J, Weiss A (2001) Identification of the minimal tyrosine residues required for linker for activation of T cell function. *J Biol Chem* 276:29588–29595.
6. Houtman JC, *et al.* (2004) Binding specificity of multiprotein signaling complexes is determined by both cooperative interactions and affinity preferences. *Biochemistry* 43:4170–4178.
7. Hartgroves LC, Lin J, Langen H, Zech T, Weiss A, Harder T (2003) Synergistic assembly of linker for activation of T cells signaling protein complexes in T cell plasma membrane domains. *J Biol Chem* 278:20389–20394.
8. Seet BT, *et al.* (2007) Efficient T-cell receptor signaling requires a high-affinity interaction between the Gads C-SH3 domain and the SLP-76 RxxK motif. *EMBO J* 26:678–689.
9. Qi Q, August A (2007) Keeping the (kinase) party going: SLP-76 and ITK dance to the beat. *Sci STKE* 2007:pe39.
10. Chardin P, *et al.* (1993) Human Sos1: A guanine nucleotide exchange factor for Ras that binds to GRB2. *Science* 260:1338–1343.
11. Freedman TS, *et al.* (2006) A Ras-induced conformational switch in the Ras activator Son of sevenless. *Proc Natl Acad Sci USA* 103:16692–16697.
12. Boykevisch S, *et al.* (2006) Regulation of ras signaling dynamics by Sos-mediated positive feedback. *Curr Biol* 16:2173–2179.
13. Margarit SM, *et al.* (2003) Structural evidence for feedback activation by Ras. GTP of the Ras-specific nucleotide exchange factor SOS. *Cell* 112:685–695.
14. Rhee SG, Suh PG, Ryu SH, Lee SY (1989) Studies of inositol phospholipid-specific phospholipase C. *Science* 244:546–550.
15. Ebinu JO, *et al.* (2000) RasGRP links T-cell receptor signaling to Ras. *Blood* 95:3199–3203.
16. Gillespie DT (1977) Exact stochastic simulation of coupled chemical reactions. *J Phys Chem* 81:2340–2361.
17. Fujisawa T, *et al.* (1994) The hydration of Ras p21 in solution during GTP hydrolysis based on solution X-ray scattering profile. *J Biochem* 115:875–880.
18. Sloan-Lancaster J, *et al.* (1998) ZAP-70 association with T cell receptor zeta (TCRzeta): Fluorescence imaging of dynamic changes upon cellular stimulation. *J Cell Biol* 143:613–624.
19. Swaminathan R, Hoang CP, Verkman AS (1997) Photobleaching recovery and anisotropy decay of green fluorescent protein GFP-S65T in solution and cells: Cytoplasmic viscosity probed by green fluorescent protein translational and rotational diffusion. *Biophys J* 72:1900–1907.
20. Fujiwara T, Ritchie K, Murakoshi H, Jacobson K, Kusumi A (2002) Phospholipids undergo hop diffusion in compartmentalized cell membrane. *J Cell Biol* 157:1071–1081.
21. Altan-Bonnet G, Germain RN (2005) Modeling T cell antigen discrimination based on feedback control of digital ERK responses. *PLoS Biol* 3:e356.
22. Fujioka A, *et al.* (2006) Dynamics of the Ras/ERK MAPK cascade as monitored by fluorescent probes. *J Biol Chem* 281:8917–8926.
23. Bhalla US, Iyengar R (1999) Emergent properties of networks of biological signaling pathways. *Science* 283:381–387.

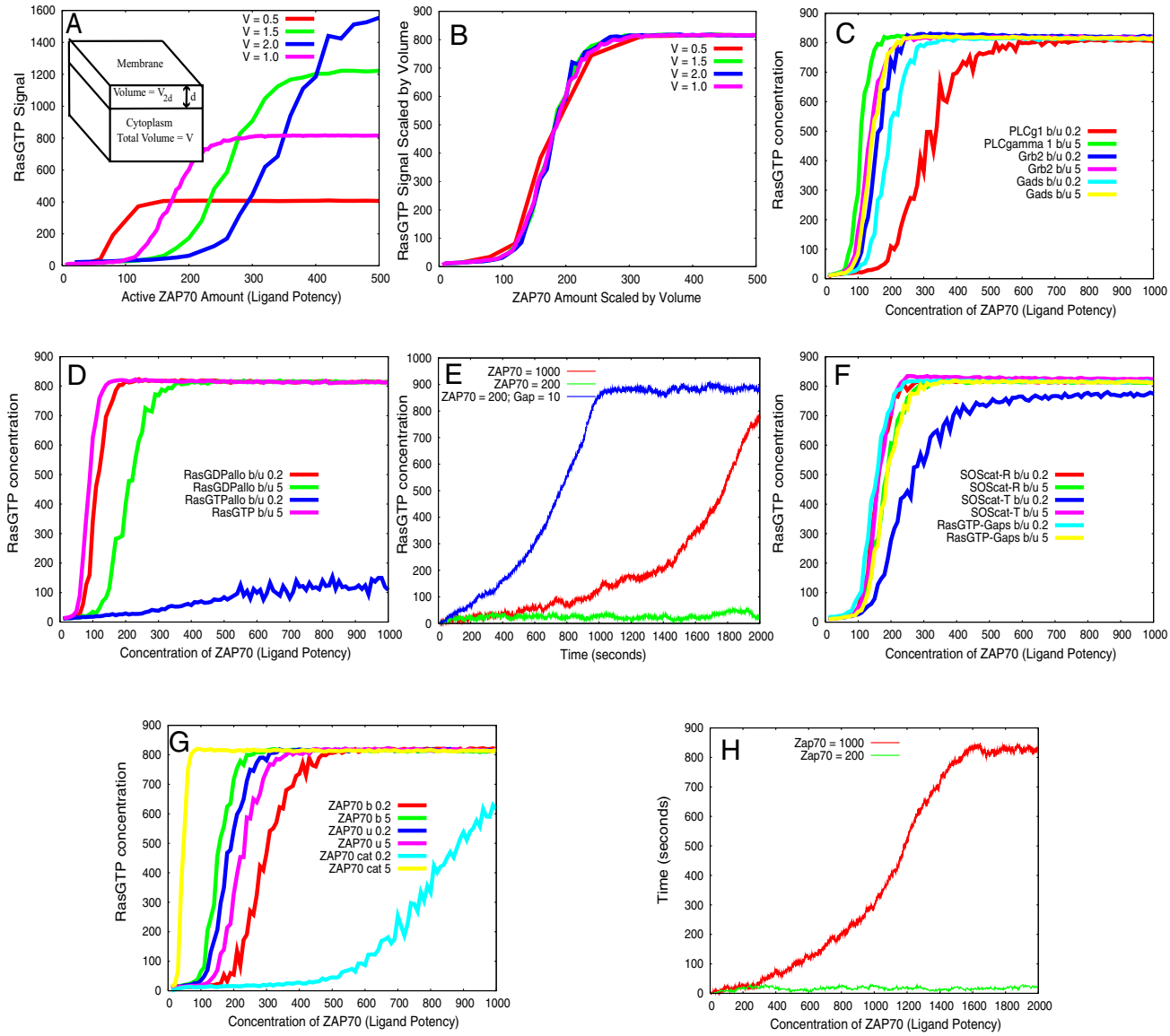

Fig. S1. (*A*) RasGTP activation levels plotted against signal strength with choice of different simulation volumes. V = 1.0 refers to the base case discussed in the article, whereas V = 0.5 is half the base case volume, V = 1.5 is one and one half times the base case volume, and so on. The results show that changing the volume changes the threshold amount of ZAP70 required for initiation of the positive feedback loop and activation of all of the RasGDP in the simulation box. *Inset* shows a schematic of the simulation box. (*B*) RasGTP activation with different simulation volumes scaled by volume factor. To test whether there is any qualitative difference between the reaction kinetics of the different simulation boxes, we scaled the number of molecules in the simulation box by the volume factor and plotted the scaled RasGTP vs. scaled ZAP70. All of the curves fall on the same line, showing that there is no qualitative difference between these simulation volumes (i.e., the same concentration of ZAP70 is required for the same concentration of activated Ras in all cases). (*C*) Sensitivity of the total RasGTP signal to the LAT binding−unbinding parameters are plotted. Binding−unbinding of PLCγ1, Grb2, or Gads on LAT does not affect the qualitative behavior of the model. (*D*) Sensitivity to RasGDP or RasGTP binding to allosteric site of Grb2/SOS. Binding−unbinding of RasGDP or RasGTP to the allosteric site of Grb2/SOS does not affect the qualitative behavior of the RasGTP signal except when the binding−unbinding rate of RasGTP is decreased by 5. This results in Grb2/SOS being preferentially bound to RasGDP, and it delays the initiation of the positive feedback, as can be seen in the next panel. (*E*) Signal timing for low binding–unbinding rates of RasGTP to SOS allosteric site. When the binding of RasGTP to the allosteric site of SOS is weakened, it preferentially increases the relative propensity of RasGDP binding to SOS. Because SOS is preferentially occupied with RasGDP, the output of RasGTP is slower. This pushes the threshold to the right and increases the time taken to achieve maximal activation (red curve). Decreasing the effective threshold by decreasing the concentration of RasGAPs, for example, leads to maximal activation much earlier (blue line). (*F*) Sensitivity of RasGDP binding to the catalytic site of Grb2/SOS and RasGAPs. Binding–unbinding of RasGDP to the catalytic site of SOS or to RasGAPs does not affect the qualitative behavior of the signal. (*G*) Sensitivity to parameters involved in the phosphorylation of LAT. Binding–unbinding and catalytic rates of ZAP70 do not qualitatively affect the RasGTP signal except when catalytic rates of ZAP70 phosphorylating LAT are reduced by a factor of 5. In this case the positive feedback loop is ignited, but sharpness seems somewhat abrogated. This is because the initiation of the positive feedback is slower than before, as is demonstrated in the next panel. (*H*) RasGTP signal timing when ZAP70 catalytic rate is decreased by 5. Decreasing the catalytic rate of ZAP70 increases the signal threshold required to ignite the positive feedback loop and increases the time required. Thus the signal level of ZAP70 = 200 shows no activation in 2,000 s (green line). However, the signal level of ZAP70 = 1000 (red line) shows a delayed activation, reaching maximal value at approximately 1,600 seconds. Consequently this change does not change the consequences of the model qualitatively; all it changes is the appropriate time window of measurement.

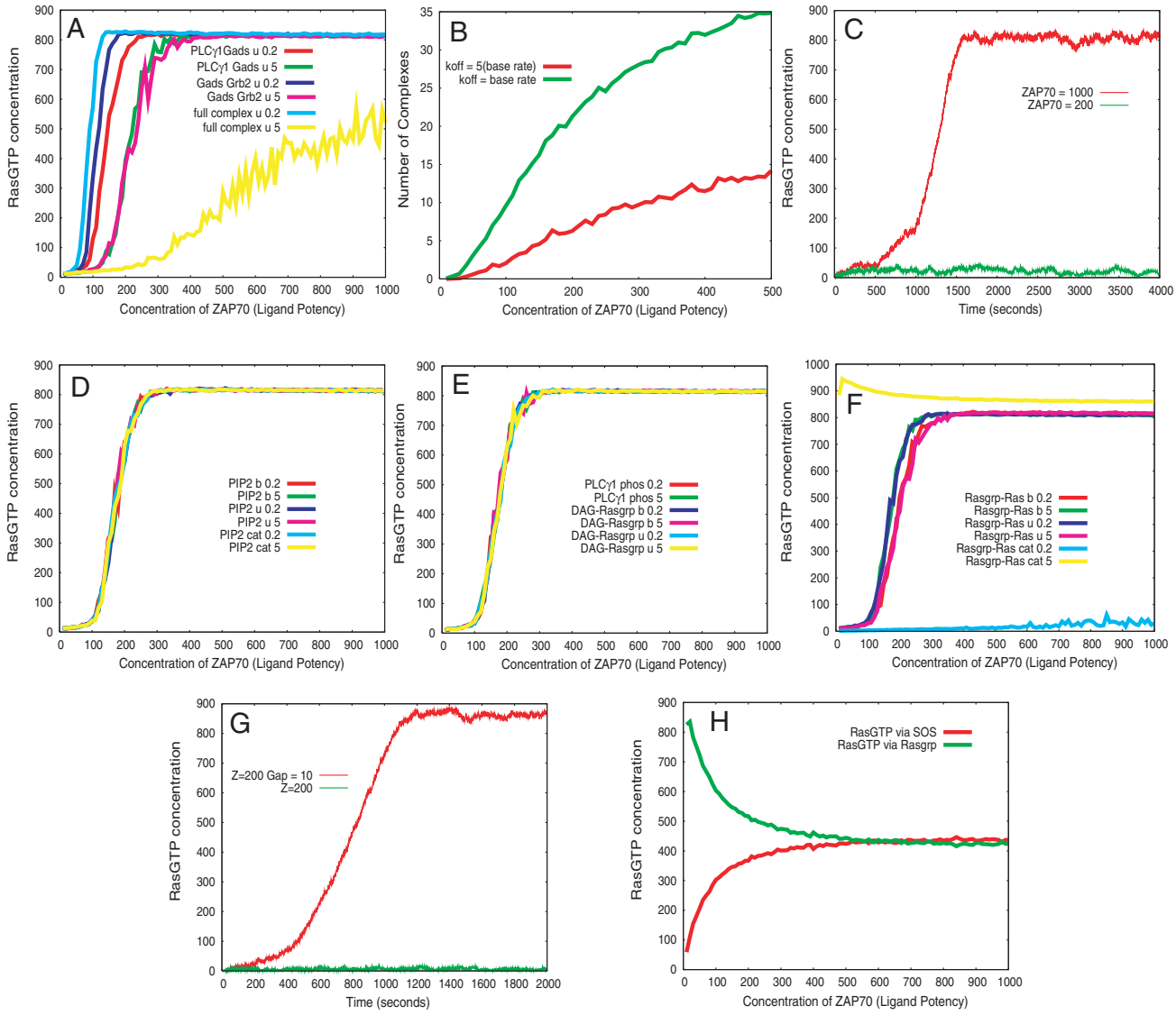

Fig. S2. (*A*) Sensitivity of parameters involved in complex assembly on LAT. The unbinding rate of the full complex represents the degree of cooperativity. Increasing this unbinding rate is tantamount to decreasing cooperativity and leads to a change in the RasGTP signal at the time measured. The dissociation rates of the partial complexes do not have a qualitative effect on the signal. However, when the dissociation rate of the complete complexes increases, complex formation decreases significantly. (*B*) Complex formation decreases significantly when cooperativity decreases. The unbinding rate of complete complexes sets the level of cooperativity in complex formation. Decreasing the level of cooperativity leads to a smaller number of ideal complexes formed. This may keep stably bound SOS below threshold or slow down maximal activation. For our simulation, a larger signal is needed to produce enough SOS at the membrane, which also requires more time (because it is bound weaker) to ignite the positive feedback loop. (*C*) Signal timing for weaker cooperativity. When cooperativity is weakened by increasing the off-rate for the unbinding of the complete complex by a factor of 5, the positive feedback loop does not ignite even at long times (green curve). The signal strength is above the base case threshold. However, if the signal strength is increased fivefold to 1,000, the positive feedback loop ignites (red curve) in a manner similar to the base case. (*D*) Sensitivity to parameters involved in the hydrolysis of PIP2. Binding–unbinding rates of PIP2 with activated PLCγ1 and catalytic rates of PLCγ1 do not affect the RasGTP signal at all. (*E*) Sensitivity to rates of DAG production and RasGRP activation. Phosphorylation rate of PLCγ1, as well as binding–unbinding rates of DAG with RasGRP, do not affect the RasGTP signal. (*F*) Sensitivity to rates involved in Ras activation by RasGRP. Only the catalytic rate of RasGRP affects the RasGTP signal, whereas changes in the binding–unbinding rates of Ras to RasGRP have no effect. (*G*) RasGTP vs. time when Rasgrp1 catalytic rate is decreased by a factor of 5. RasGTP is required for priming the feedback loop. At low catalytic rates, therefore, enough RasGTP cannot accumulate, given the RasGAP concentration in the simulation box, to prime the feeedback loop (green line). A small decrease in the concentration of RasGAPs restores Ras activation for these parameter values (red line). (*H*). RasGTP at high RasGRP catalytic rates. When the catalytic rate of Rasgrp1 is higher by a factor of 5, it is larger than the highest catalytic rate of SOS. Because RasGRP gets activated before SOS does, it converts most of the RasGDP into RasGTP at low signal. As the signal strength increases, the weights of the two pathways become equal. Note that SOS behaves as if it is only in its high catalytic rate state because there is enough RasGTP generated by RasGRP by the time SOS has assembled on the membrane.

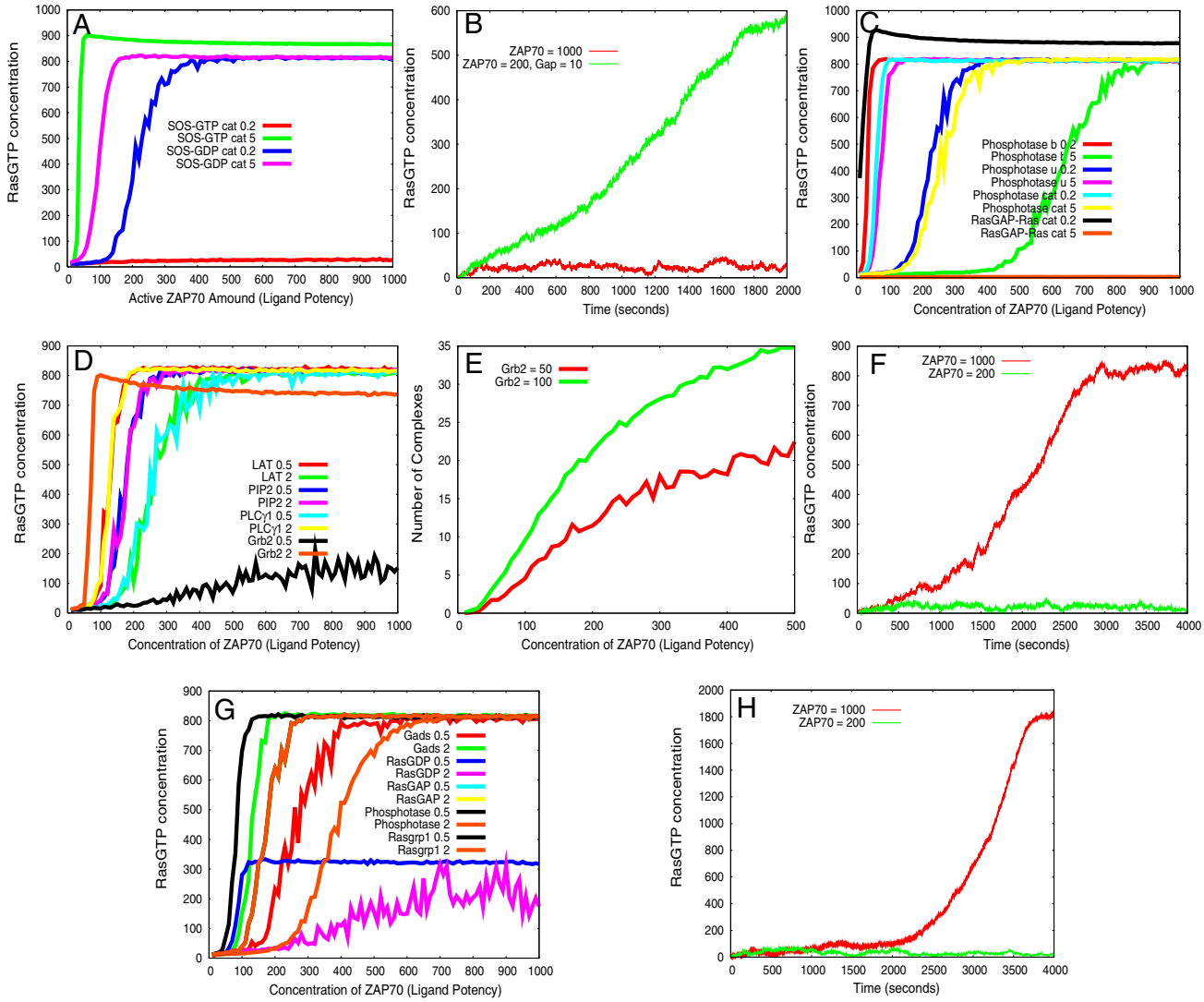

Fig. S3. (*A*) Sensitivity to parameters of the catalytic rates of SOS are shown. Changes in the catalytic rate of SOS lead to the same activation profile as in the base case, but with changes in the threshold and the sharpness of the Ras activation curve. The exception is when the catalytic rate of RasGTP bound SOS is decreased fivefold. Because this rate, along with the binding affinity of RasGTP to SOS, is what causes the positive feedback in the first place, it is not surprising that large changes in this rate have significant effects. Because the rate of SOS-RasGTP catalysis (0.008 s^{-1}) is still greater than that of SOS-RasGDP (0.003 s^{-1}), we should expect a weaker positive feedback. However, this is at a higher threshold in terms of stably bound SOS molecules than achievable in the simulation box. Changing the concentration of RasGAPs decreases this threshold and restores the positive feedback loop, although it takes longer to achieve maximal activation of RasGTP. (*B*) Timing of signal when positive feedback is weaker. A ZAP70 signal of 1000 molecules does not maximally activate RasGTP. However, decreasing the concentration of RasGAPs restores maximal activation even at Zap70 = 200. This is still at later times than the base case. (*C*) Sensitivity to parameters involved in LAT dephosphorylation and GTPase rate of RasGAPs are plotted. Changes in binding–unbinding rates and catalytic rates of the phosphatase change the threshold of the signal and have some effect on the sharpness but do not lead to a qualitative change. Increase of the GTPase activity of RasGAPs fivefold suppresses the RasGTP signal. This is similar to the effect of increasing concentration discussed elsewhere. (*D*) RasGTP signal with changes in concentration of LAT, PIP2, PLCγ1, and Grb2. Except for Grb2/SOS, changes in other concentrations shown here have no effect on the qualitative behavior of the model. The former effect is because at this reduced concentrations, lower levels of Grb2/SOS stably accumulate at the PM, shown in the next panel. (*E*) Complex formation when Grb2-SOS concentration is decreased is shown. The number of complete complexes is less at any signal when the Grb2-SOS concentration is decreased. (*F*) Timing of signal when concentration of Grb2-SOS is reduced to half. Because complex formation is hampered as shown above, a stronger signal is needed to ignite positive feedback. The positive feedback loop cannot ignite at ZAP70 = 200 (green line), which is above the threshold in the base case. However, it can ignite at ZAP70 = 1000 (red line), although at a later time window. (*G*) RasGTP signal with changes in concentration of Gads, RasGDP, RasGAPs, phosphatase, and Rasgrp1. Only the concentrations of RasGDP and of RasGAPs affect the qualitative behavior of the RasGTP signal. Changes in other species concentrations have no effect. (*H*) Signal timing when RasGDP concentration has increased 2 times. Increasing RasGDP concentration increases the propensity of Grb2-SOS being occupied by RasGDP. Hence it increases the threshold and the activation time of the signal (red curve).

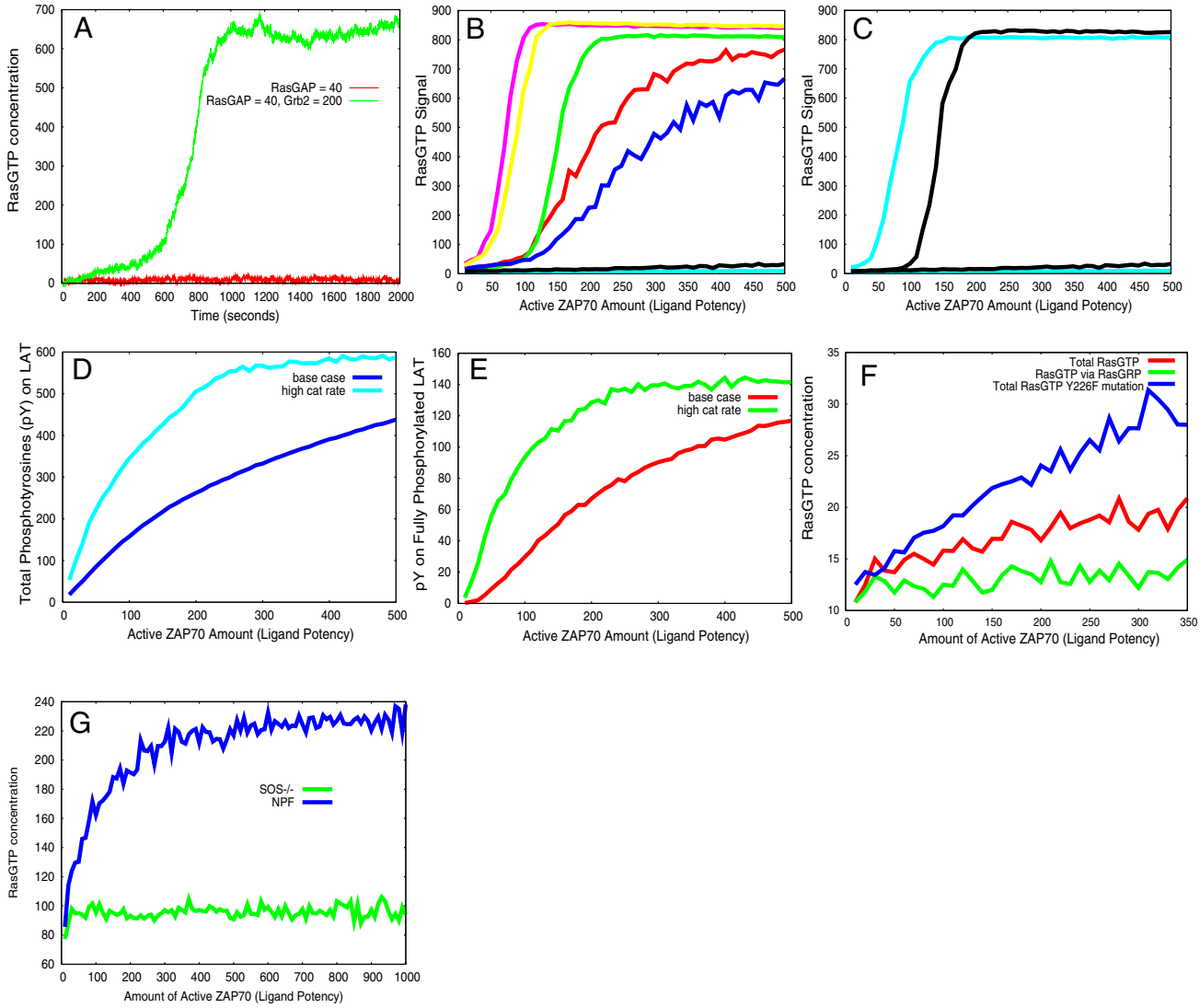

Fig. S4. (*A*) Signal timing when RasGAP concentration is doubled. As in the case when the catalytic rates of RasGAPs are increased fivefold, doubling of RasGAP concentration leads to suppression of RasGTP production even at high signal (red line, ZAP70 = 1000). This is because the threshold required for igniting the positive feedback loop is larger than the maximal number of stably bound SOS at these concentrations. Hence increasing the concentration of Grb2-SOS to enable accumulation of more complexes and more transiently bound Grb2-SOS restores the activation of the positive feedback loop. (*B*) Changes in multiple parameter values. Seven representative plots of 20 simulations performed by randomly changing all parameter values by 20% are shown. When the catalytic activity of RasGAP is strengthened but the higher SOS catalytic rate is weakened, it only affects the timing of maximal Ras activation (red and blue curves), hence there is no qualitative change in the model. However, when the RasGRP catalytic rate is also reduced, we find that there is insufficient Ras activity to prime the SOS feedback loop, and Ras activation remains at very low levels (black and light blue curves). Changes that decrease the catalytic activity of RasGAPs have no qualitative effect on the activation of Ras (green curve), but if accompanied by an increase in the RasGRP and the SOS catalytic rate can reduce the threshold for the positive feedback loop (pink and yellow curves). (*C*) Restoring basal RasGAP parameters restores Ras activation. The two curves of *B* that showed no activation are replotted along with simulations of the system with the same parameter values except for the RasGAP parameters, which were left at the basal values. In both cases maximal activation of Ras is restored. The difference in threshold arises from the higher catalytic rate of both RasGRP and SOS for the light blue curve. Thus we require that the GTPase activity of the RasGAPs does not abrogate Ras signaling through RasGRP, otherwise the SOS feedback loop cannot be primed. (*D*) Total phosphotyrosines on LAT with higher catalytic rate of ZAP70 than the base case show a sharper increase as a function of signal strength. The sharpness of the increase is set by the catalytic rates of phosphorylation and dephosphorylation. Here we show that a fivefold higher rate of phosphorylation leads to a steeper increase in total pY on LAT (light blue line) compared with the base case (dark blue line). (*E*) Fully phosphorylated LAT also shows a sharper rise as a function of signal strength, at a higher catalytic rate of ZAP70 than the base case (red line). (*F*) RasGTP activation after a mutation abrogating positive feedback in SOS is a graded function of signal strength. The Y226F mutation is shown for comparison. (*G*) RasGTP activation for the SOS-/- and the no-positive-feedback mutation at a lower RasGAP catalytic rate is shown. At a lower RasGAP activity, which may be relevant if RasGAP activity is dynamically modulated, the mutation without positive feedback in SOS shows a graded response to increasing signal strength (blue curve). The $SOS^{-/-}$ curve (green) is shown for comparison.

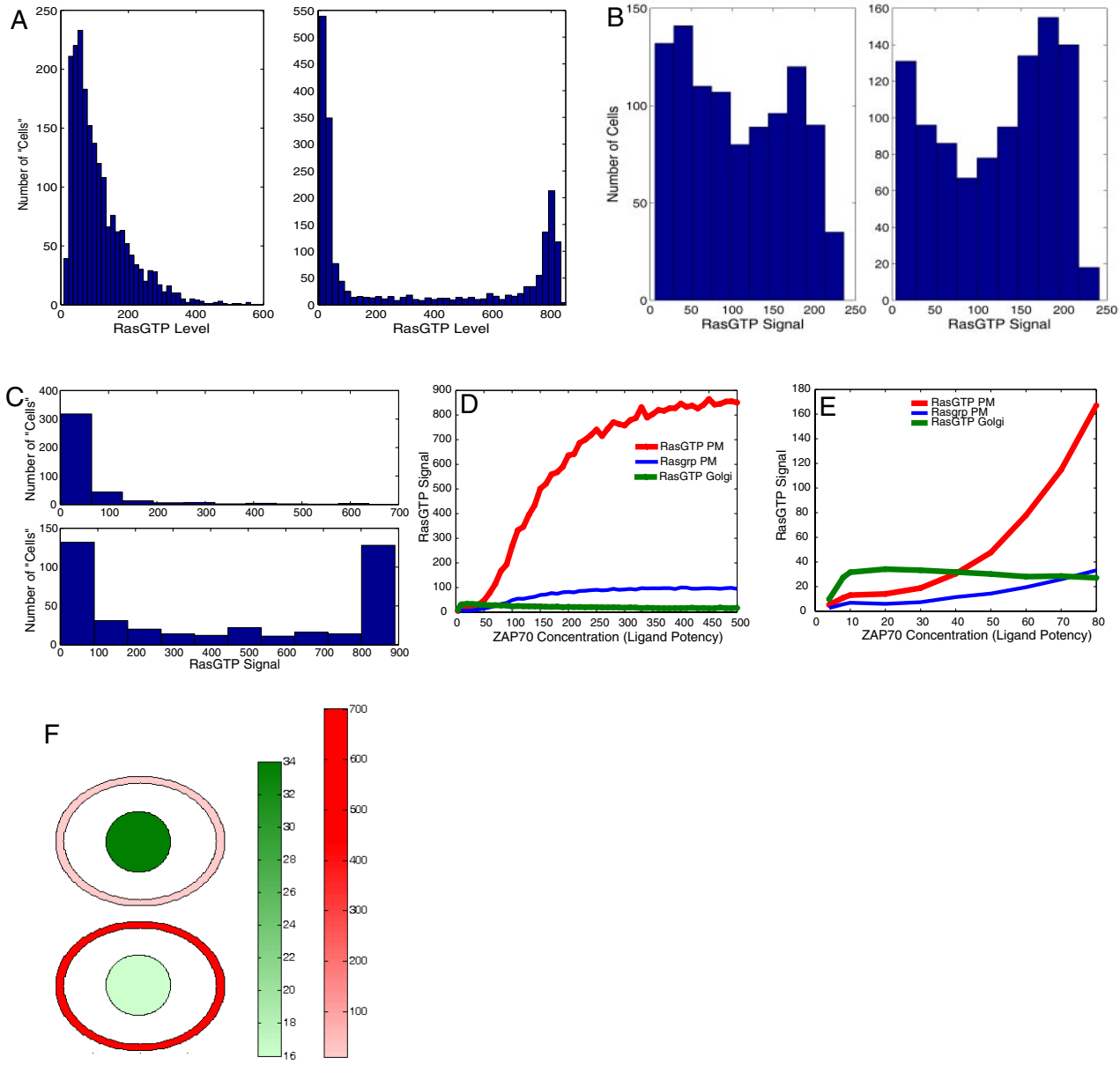

Fig. S5. (*A*) Bimodality in the RasGTP signal shown for the base case. For these parameter values, at the time window of 20 min and a signal strength of 130 molecules of ZAP70, the distribution of RasGTP is still unimodal but has developed a long tail (left panel). At 50 min, however, the distribution of the RasGTP signal is bimodal. Thus the model displays bimodality of the RasGTP signal, in accord with experimental observations, but at the parameter values chosen its timing is delayed. (*B*) Reducing the initial concentration of RasGDP in the simulation box reduces the time at which bimodality can be observed to 25 min (Zap70 = 150; *Left* is at 20 min, *Right* is at 25 min). (*C*) Changing the catalysis rate of RasGTP bound SOS by a factor of 5 decreases the time to observe bistability to 8 min (Zap70 = 150, *Bottom*). At 60 seconds bistability has not yet developed (*Top*). (*D*) RasGTP activation in the compartment model described in the SI Text. The compartment model shows the sharp response to ligand potency due to the SOS feedback loop as before (red line). The contribution of the RasGRP pathway on the plasma membrane is the blue curve. The positive selection signal on the Golgi is stronger at smaller signal strengths than the signal at the plasma membrane. Interestingly, the signal at the Golgi declines at higher signal strengths, owing to competition between the PM and the Golgi for activated RasGRP. This qualitatively matches what is seen in experiment. The RasGTP signal in this case is measured at 11 min. The reason for the shorter time despite all parameters remaining the same as in the basic model is the lower constitutive concentration of RasGAPs in this model. (*E*). Positive selection in the compartment model is indicated by a blow-up of the low signal region. The RasGTP activation at the Golgi is robust at low signal strength, whereas the RasGTP activation on the plasma membrane is strongly suppressed. Once the positive feedback loop in Ras activation by SOS at the plasma membrane is ignited, Ras activation at the Golgi declines, and RasGTP at the plasma membrane dominates. (*F*) Spatial compartmentalization of RasGTP activation is a consequence of the compartment model. The central elliptical body represents the Golgi, whereas the surrounding ring represents the plasma membrane. This is an *in silico* prediction of a fluorescent imaging experiment. The intensities of the colors represent the concentrations of RasGTP and have been calculated using inbuilt routines of MATLAB. Positive selection leads to the Golgi becoming florescent, whereas the plasma membrane is dim. Negative selection leads to a firestorm of florescence on the plasma membrane, whereas the Golgi dims.

Table S1. Chemical reactions and parameters used for simulations

Reaction	k_{on} $\mu M^{-1}s^{-1}$	k_{off} s^{-1}	K_d μM (measured value if any)	k_{cat} s^{-1} (measured value if any)
Zap70 binding, unbinding to Lat tyrosines(Y)	0.204	1.0	4.9	
Bound Zap70 phosphorylates Lat Y				1.0
Lat pY132 binding, unbinding to PLCγ1	7.92	0.5	0.063 (0.062) Ref. (6)	
Lat pY191 binding, unbinding to Grb2	6.24	0.5	0.08 (0.079) Ref. (6)	
Lat pY226 binding, unbinding to Grb2	6.24	1.1	0.176 (0.174) Ref. (6)	
Lat pY191 binding, unbinding to Gads	5.28	0.8	0.152 (0.152) Ref. (6)	
Lat pY226 binding, unbinding to Gads	5.28	2.2	0.417 (0.410) Ref. (6)	
Activation of PLCγ1 by Gads (on Lat)				5.0
Unbinding of Gads or PLCγ1 from Lat when Gads is bound to pY191 (Grb2/SOS not on pY226)		0.08		
Unbinding of Gads or Grb2 from LAT when Gads is on pY191 and Grb2 on pY226 (PLCγ1 not on pY132)		0.1		
Unbinding of PLCγ1 or Gads or Grb2 when PLCγ1 is on pY132, Gads on pY191 and Grb2 on pY226		0.01		
RasGDP binding, unbinding to allosteric site on Grb2/SOS	0.102	3.0	29.4 (24.5) Ref. (11, 12, 21)	
RasGTP binding, unbinding to allosteric site on Grb2/SOS	0.102	0.4	3.92 (3.6) Ref. (11, 12, 21)	
RasGDP binding, unbinding to catalytic site on Grb2/SOS which has RasGDP on allosteric site	0.04	1.0	24.51 (25) Ref. (11, 12, 21)	
RasGDP binding, unbinding to catalytic site on Grb2/SOS which has RasGTP on allosteric site	0.06	0.1	1.67 (1.9) Ref. (11, 12, 21)	
Grb2/SOS with RasGDP on allosteric site activates RasGDP on catalytic site				0.003 (0.003) Ref. (11, 12, 21)
Grb2/SOS with RasGTP on allosteric site activates RasGDP on catalytic site				0.04 (0.038) Ref. (11, 12, 21)
PIP2 binds to PLCγ1 on Lat	4.08	1.0	0.245	
PLCγ1 hydrolyses PIP2 to form DAG and IP3				0.5
DAG binding, unbinding to RasGRP	4.08	0.08	0.02	
RasGRP binding, unbinding to RasGDP	0.32	1.0	3.1 (3) Ref. (22) Measurement for RasGRF1	
RasGRP bound to RasGDP activates Ras				0.01 (0.01) Ref. (22) Measurement for RasGRF1
pY on Lat binding, unbinding to phosphatase	2.4	1.0	0.416	
pY on Lat dephosphorylated by bound phosphatase				2.0
RasGAP binding, unbinding with RasGTP	2.4	1.0	0.416 Ref. (23) Measured values range from 0.1–5 μM	
RasGAP bound to RasGTP deactivates RasGTP				0.1 (0.1) Ref. (24, 25) Value for WT p120 RasGAP measured under nonsaturating conditions.
ZAP70 Decays		0.01		
Lat with only pY132 dephosphorylates		1		

Reference numbers follow those given in the SI Text.

Table S2. Concentrations used in simulations

Species	No. of molecules in V	Effective concentration
ZAP70 (activated)	1–1,000	12.5–12,500 molecules/μm^3
LAT	1,000	250 molecules/μm^2
Grb2	100	1,250 molecules/μm^3
RasGDP	1,000	250 molecules/μm^2
Gads	100	1,250 molecules/μm^3
PLCγ1	100	1,250 molecules/μm^3
Rasgrp1	50	625 molecules/μm^3
PIP2	5,000	1,250 molecules/μm^2
RasGAPs	20	250 molecules/μm^3
Phosphotase	500	6,250 molecules/μm^3

Note that Grb2/SOS is regarded as a single species in the computational model. Hence concentration of SOS is the same as the concentration of Grb2 above.

Table S3. Sensitivity analysis of parameters

	Parameters	Variation	Decrease by 5	Increase by 5
1	Lat pY132 binding, unbinding with PLCγ1 (noncooperative)	Constrained	Increase in threshold, decrease in sharpness. (Fig. S1*C*)	Decrease in threshold. Sharper (Fig. S1*C*)
2	LAT pY191 and pY226 binding, unbinding with Grb2/SOS (noncooperative)	Constrained	No qualitative change (Fig. S1*C*)	Small decrease in threshold (Fig. S1*C*)
3	LAT pY191 and pY226 binding, unbinding with Gads (noncooperative)	Constrained	No qualitative change (Fig. S1*C*)	Small decrease in threshold (Fig. S1*C*)
4	RasGDP binding, unbinding with the allosteric site on Grb2/SOS on LAT	Constrained	Small decrease in threshold (Fig. S1*D*)	Very small increase in threshold (Fig. S1*D*)
5	RasGTP binding, unbinding with the allosteric site on Grb2/SOS on LAT	Constrained	Decreasing the rate at which RasGTP binds to the allosteric site of SOS weakens the positive feedback loop. As a result it requires more SOS and more time to reach maximal Ras activation (Fig. S1 *D* and *E*)	Threshold decreased. Sharper (Fig. S1*D*)
6	RasGDP binding, unbinding to catalytic site of Grb2/SOS with RasGDP on allosteric site	Constrained	No change (Fig. S1*F*)	No change (Fig. S1*F*)
7	RasGDP binding, unbinding to catalytic site of Grb2/SOS with RasGTP on allosteric site	Constrained	Decrease in sharpness (Fig. S1*F*)	No change (Fig. S1*F*)
8	RasGTP binding, unbinding to RasGAP	Constrained	Small decrease in threshold (Fig. S1*F*)	Small increase in threshold (Fig. S1*F*)
9	Tyrosine sites on LAT binding with ZAP70	Independent	Threshold increases; sharpness decreases (Fig. S1*G*)	No qualitative change (Fig. S1*G*)
10	Tyrosine sites on LAT bound with ZAP70 dissociating into free LAT and free ZAP70	Independent	No change (Fig. S1*G*)	Small increase in threshold (Fig. S1*G*)
11	ZAP70 bound to tyrosine sites on LAT phosphorylating them and dissociating.	Independent	Decrease in the catalytic rate of phosphorylation by ZAP70 increases the threshold required for initiation of the positive feedback significantly, and increases the time taken for full activation. The latter is manifested in a less steep threshold (Fig. S1 *G* and *H*)	Large decrease in threshold. Sharper response (Fig. S1*G*)
12	Dissociation of complex on LAT containing PLCγ1 bound to pY132 and Gads bound to pY191 (without Grb2/SOS on pY226)	Independent	Threshold increases to over 300. Sharpness decreases (Fig. S2*A*)	Threshold decreases to $\approx$100 (Fig. S2*A*)
13	Dissociation of complex on LAT containing Gads bound to pY191 and Grb2/SOS on pY226 (without PLCγ1 on pY132)	Independent	Threshold decreases slightly (Fig. S2*A*)	Minor shift in threshold and decrease in sharpness (Fig. S2*A*)
14	Dissociation of complex on LAT with PLCγ1 on pY132, Gads on pY191, and Grb2 on pY226	Independent	Threshold decreases to $\approx$50 (Fig. S2*A*)	The faster rate of complex dissociation decreases stably bound Grb2/SOS on the membrane. This means that higher signals and more time is needed for ignition of the positive feedback loop (Fig. S2 *A*–*C*)
15	PIP2 binds to activated PLCγ1 on LAT	Independent	No change (Fig. S2*D*)	No change (Fig. S2*D*)
16	PIP2 unbinds from activated PLCγ1	Independent	No change (Fig. S2*D*)	No change (Fig. S2*D*)
17	PLCγ1 bound to PIP2 hydrolyses PIP2 forming DAG, IP3, and free PLCγ1	Independent	No change (Fig. S2*D*)	No change (Fig. S2*D*)
18	Gads bound to pY191 on LAT activates PLCγ1 on pY132	Independent	No change (Fig. S2*E*)	No change (Fig. S2*E*)
19	RasGRP binds to DAG forming the activated species RasGRP-DAG	Independent	No change (Fig. S2*E*)	No change (Fig. S2*E*)
20	RasGRP-DAG dissociates into free RasGRP and free DAG	Independent	No change (Fig. S2*E*)	No change (Fig. S2*E*)
21	RasGRP-DAG binds RasGDP	Independent	No change (Fig. S2*F*)	No change (Fig. S2*F*)
22	RasGDP dissociates from RasGRP-DAG bound to RasGDP	Independent	No change (Fig. S2*F*)	No change (Fig. S2*F*)
23	RasGDP bound to RasGRP-DAG is converted into RasGTP and free RasGRP-DAG	Independent	Production of RasGTP by RasGRP primes the SOS feedback loop. With a weaker catalytic rate for RasGRP, it takes a longer time for initiation of the positive feedback (Fig. S2 *F* and *G*)	This value of the parameter makes the catalytic rate of RasGRP faster than the higher rate of SOS. Because RasGRP is activated fully at low signals, all the Ras*GDP* in the simulation box gets activated by RasGRP even at low signals (Fig. S2 *F* and *H*)
24	Catalytic conversion of RasGDP into RasGTP by Grb2/SOS with RasGDP on its allosteric site	Independent	Negligible change (Fig. S3*A*)	Decrease in threshold (Fig. S3*A*)

	Parameters	Variation	Decrease by 5	Increase by 5
25	Catalytic conversion of RasGDP into RasGTP by Grb2/SOS with RasGTP on its allosteric site	Independent	Delays the initiation of the positive feedback loop and increases the threshold (Fig. S3 *A* and *B*)	Threshold shifts close to 0. Very sharp (Fig. S3*A*)
26	Phosphatase binds to phosphorylated tyrosine residues (pY) on LAT	Independent	Threshold decreases to near 0. Sharper (Fig. S3*C*)	Large increase in threshold to ≈600. Sharpness decreased (Fig. S3*C*)
27	Phosphatase bound to pY on LAT unbinds	Independent	Threshold decreases to ≈50. Sharper (Fig. S3*C*)	Small increase in threshold and decrease in sharpness (Fig. S3*C*)
28	Phosphatase bound to pY on LAT dephosphorylates the tyrosine residue and dissociates from LAT	Independent	Small increase in threshold to over 200 (Fig. S3*C*)	Decrease in threshold to ≈50 (Fig. S3*C*)
29	RasGAP bound to RasGTP catalyzes it into RasGDP and dissociates	Independent	Threshold close to zero (Fig. S3*C*)	Ras activation is suppressed. Initiation of the positive feedback loop now requires more SOS molecules than are present in the simulation box (Fig. S3*C*)

Table S4. Parameter sensitivity analysis of mutations

Reactions	Increase rate by 5	Decrease rate by 5
Zap70 binding–unbinding	No qualitative change	No qualitative change
PLCγ1 binding–unbinding (noncooperative)	No qualitative change	No qualitative change
Grb2/SOS binding–unbinding (noncooperative)	No qualitative change	No qualitative change except Y226F, which shows full activation qualitatively similar to the wild-type case. This is because the unbinding rate of bare Grb2/SOS on LAT is now small enough to support the initiation of the positive feedback loop.
Gads binding–unbinding (noncooperative)	No qualitative change	No qualitative change
Unbinding from partial PLCγ1-Gads complexes	No qualitative change	No qualitative change
Unbinding from complete PLCγ1-Gads-Grb2 complexes	No qualitative change	No qualitative change
RasGDP binding–unbinding to SOS allosteric site	No qualitative change	No qualitative change
RasGTP binding–unbinding to SOS allosteric site	No qualitative change except for the Y226F mutation, which shows full activation similar to wild type	No qualitative change
RasGDP binding–unbinding to SOS-RasGDP catalytic site	No qualitative change	No qualitative change, but Y226F shows a higher level of RasGTP activation
RasGDP binding–unbinding to SOS-RasGTP catalytic site	No qualitative change	No qualitative change
SOS-RasGDP catalytic rate	Activation increases for all but SOS$^{-/-}$. Y226F shows full activation qualitatively similar to wild type Significant but graded increase in activation level for NPF mutation	Activation level decreases for all but SOS$^{-/-}$
SOS-RasGTP catalytic rate	Y132F and Gads$^{-/-}$ At high signals the positive feedback loop of SOS ignites but at later times Y226F: full activation, like wild-type response Because this rate is measured, this has limited physiologic relevance. It indicates the possibility that if real *in vivo* rates are higher than the measured value, very strong self-antigens cause negative selection	No qualitative change
RasGRP catalytic rate	SOS$^{-/-}$, Y226F, and NPF mutation: maximal activation of RasGTP via the RasGRP pathway No change in others.	SOS$^{-/-}$, Y226F, and NPF mutation shows much lower activation. No change in others
Phosphatase binding, unbinding to LAT	No qualitative change	No qualitative change. However, somewhat higher levels of activation are seen for all mutations
Phosphatase catalytic rate	No qualitative change	No qualitative change, though somewhat higher levels of activation are observed. Y226F shows a significantly higher level of activation
RasGAP binding–unbinding to RasGTP	No qualitative change	No qualitative change
RasGAP catalytic GTPase rate	Very low RasGTP signal as a consequence of the very high rate of RasGAP GTPase activity for all mutations	SOS$^{-/-}$: maximal activation via RasGRP pathway at low signal Y226F: maximal activation via both pathways at low signal NPF mutation: graded response but strong activation of RasGTP Y132F & Gads$^{-/-}$: positive feedback loop in SOS can be ignited with sharp response similar to the base case. Only the SOS pathway is activated. This effect is because RasGAP's catalytic rate is an important factor in setting the threshold for activation of the SOS feedback. Lowering this threshold significantly results in activation of the positive feedback loop even in these mutations Y191F: graded response to increasing signal strength, but significantly higher levels of RasGTP activation